# LOW-LEVEL SUMMER MONSOON CIRCULATIONS *

John A. Young
University of Wisconsin
Madison, Wisconsin, U.S.A.

SUMMARY

Wind fields obtained from the Indian Ocean geostationary satellite are used to quantitatively estimate the kinematic and dynamic properties of the 900 mb summer monsoonal flow during MONEX. Mean flow results are consistent with previous expectations, including:

(a) divergence/convergence over the Arabian Sea;
(b) a region of possible inertial instability to the north of the equator over the Arabian Sea;
(c) non-conservation of absolute vorticity;
(d) a pressure field with small but important equatorial gradients;
(e) lack of quasi-geostrophic conditions within about $10^{o}$ of the equator;

Wind transients have been examined from daily, 5-day and monthly mean maps and space-time (Hovmöller type) diagrams. While some synoptic systems can be tracked, the dynamical link of winds across the equator is generally not obvious and demands careful study.

* Excerpt from report on "International Conference on Early Results of FGGE and Large-Scale Aspects of Its GARP Monsoon Experiments."

## 1. INTRODUCTION

During 1979 the Indian Ocean geostationary satellite provided exceptional coverage of cloud wind tracers, particularly during the summer monsoon months of May-July. Our research group at the University of Wisconsin (also including Drs. H. Virji, D. Wylier and programmer C. Lo) produced an atlas (Young et al, 1980) of daily winds at low and high levels which appeared to give excellent portrayal of mean and transient circulation systems. The coverage by cumulus groupings was particularly good at low levels; despite some variation in cloud tops, it appears that these "cloud winds" represent the large-scale flow near 900 mb. We are now in the research phase with this II-b data set, interpolated to a $2^{o}$ grid, and in this paper present results on the kinematics and dynamics of the mean low-level flow as well as some comments on the sampling of transient disruptions.

## 2. MEAN FLOW KINEMATICS

The best appreciation of the over-all representation is to view the mean low-level flow during July (Figure 1). Prominent are the Mascarene anti-cyclone, south-east

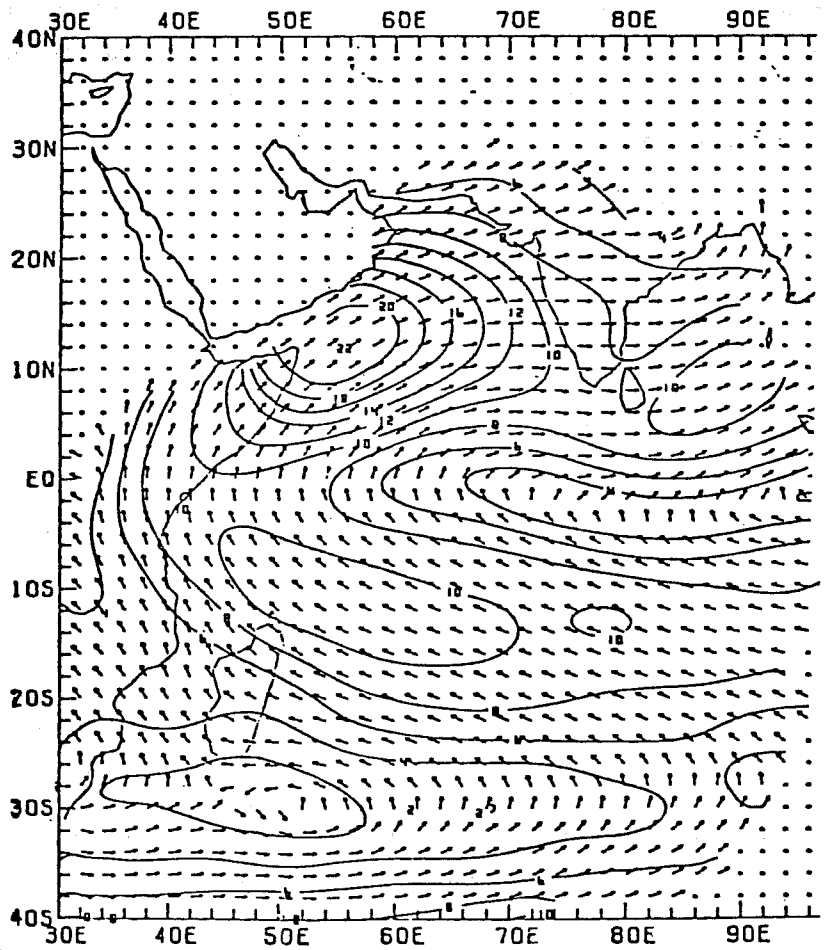


Fig. 1 Mean July monsoonal flow near 900 mb, calculated from about 20,000 cloud winds. Solid lines are isotachs (m $s^{-1}$) at 2 m $s^{-1}$ intervals, flow direction shown by vectors of unit length.

trades and "Southern Equatorial Trough" of the Southern Hemisphere, and the established southwesterly monsoon flow with a maximum near Somalia (a secondary one over the Bay of Bengal) in the Northern Hemisphere. The mean flow in May (not shown here) differs in that weak anti-cyclonic flow is found over the Arabian Sea, the maximum cross-equatorial flow is only half as large, and the southeast trades are somewhat weaker and more zonal.

Returning to the July flow, the absolute vorticity (Figure 2a) has the expected pattern arising from the large negative relative vorticity of the "gyre" flow extending from the central Arabian Sea to south of 12°S. Typical streamlines cross the equator and, in both hemispheres, show the increase of absolute vorticity along the mean trajectories. Thus, despite the success of some simple barotropic models which describe similar flows, we see that absolute vorticity is not conserved. Apparently divergence and convergence operate to produce these changes, although friction is also required near east Africa.

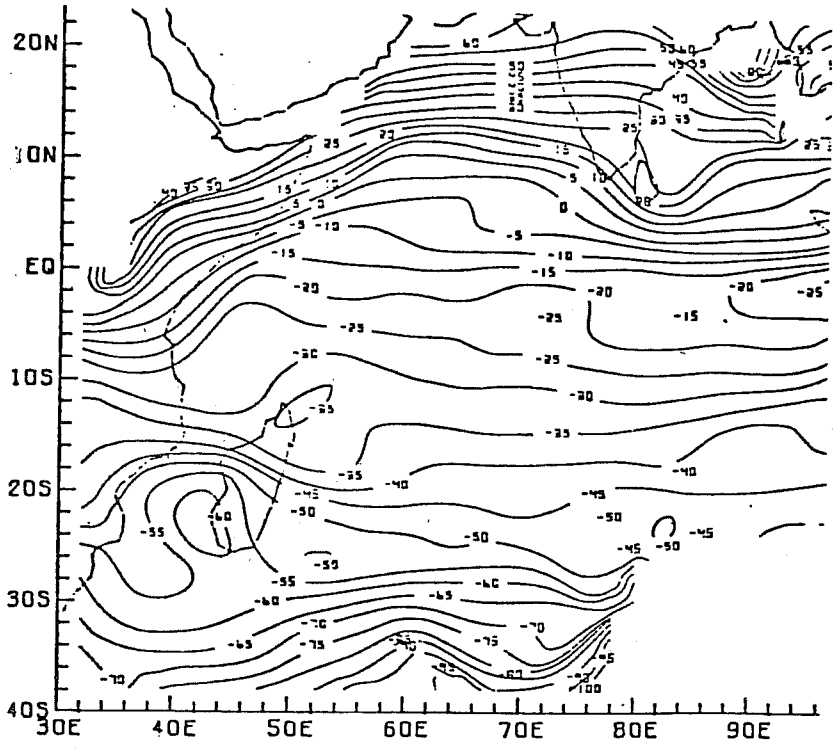


Figure 2(a) : Absolute vorticity of mean July flow shown in Fig. 1. Units are $10^{-6}$ $s^{-1}$.

The strong intensity of the circulation results in the displacement of the zero-line of absolute vorticity well into the Northern Hemisphere. According to simple theories of local (time dependent) ageostrophic perturbations, the possibility of intertial instability exists between this zero line and the equator. Lines of constant growth rate parameter (defined in the legend and negative for instability, positive for stability) are shown in Figure 2(b). The maximum values indicate a modest e-folding time of 30 hours, and correspond to the approximate time a trajectory remains within the unstable region. The exact dynamic consequences of this are unclear, since the mean flow itself is inertially accelerated; this requires theoretical investigation.

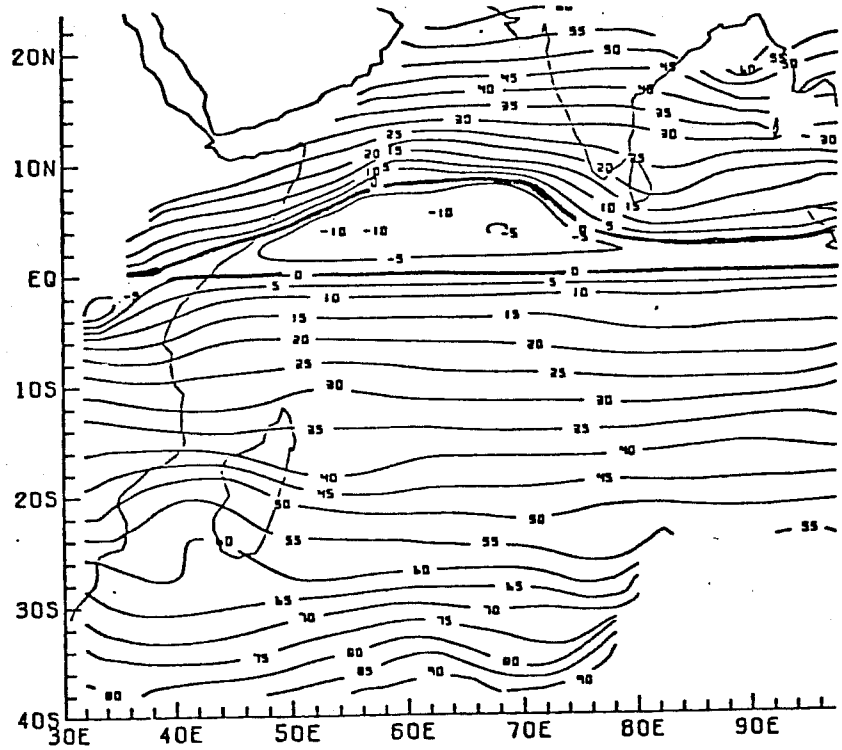


Figure 2(b) : Lines of constant inertial instability growth rate parameter, defined as sign (absolute vorticity) x $(f(\text{abs.vort.}))^{\frac{1}{2}}$, in units of $10^{-6}$ $s^{-1}$.

Finally, the mean divergence field was exhibited, but is not shown here. Weak values (less than 2 x $10^{-6}$ $s^{-1}$) were found in most of the Southern Hemisphere, with weak convergence of about this amount on the north flank of the southeast trades (due to speed convergence). To the north of the equator substantial divergence is found west of about $65^{\circ}E$; this is mainly speed divergence associated with acceleration into the Somali Jet and its flank, giving a maximum value of 10 x $10^{-6}$ $s^{-1}$. Downstream speed convergence produces values as large as -6 x $10^{-6}s^{-1}$, with smaller values (despite confluence) closer to the equator.

## 3. TRANSIENTS

The behaviour of transient departures from the mean circulation has long been of interest to researchers, ranging from long-period variations, "breaks", individual synoptic systems and possible influences advecting between hemispheres. This MONEX data set seems capable of defining some of these features. Figure 3, based upon calculations by graduate student J. Stout, shows an r.m.s. decrease from mid-latitudes toward the equator, as would be expected from baroclinic instability theory. Interestingly, the most distinct minima are found on the inward sides of the gyre's strong wind regions. A secondary maximum is found in the weak mean wind portion of the eastern Southern Equatorial Trough. No "track" of strong transient variation is found along the African coast or across the equator.

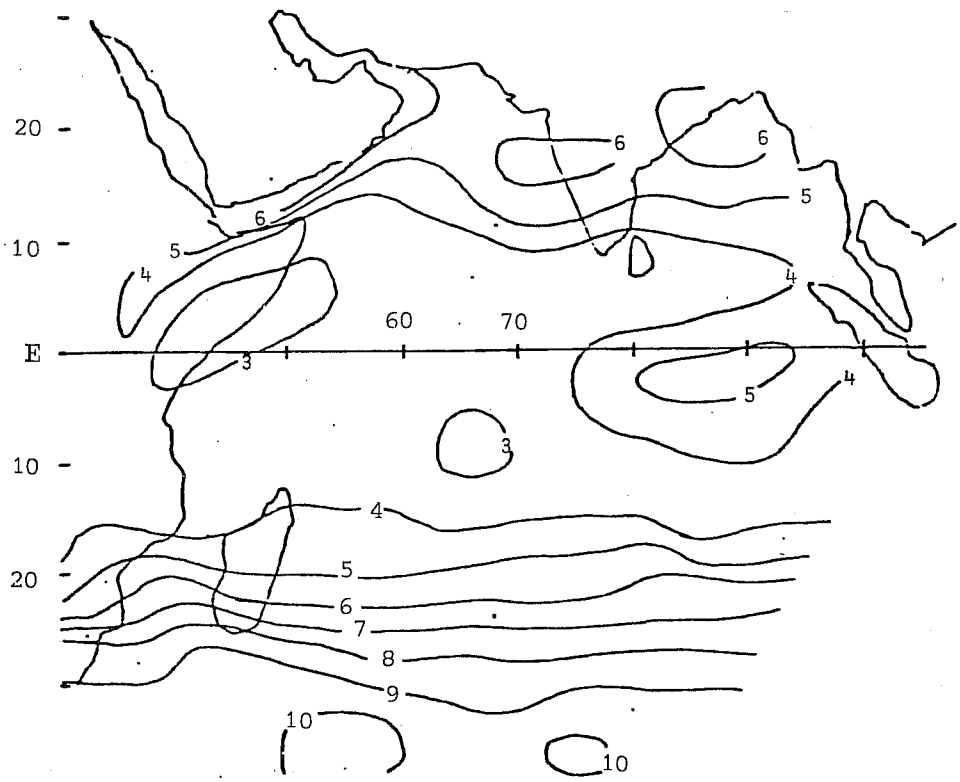


Figure 3 : R.M.S. vector wind deviations from mean established monsoon flow (16 June-31 July) at 900 mb. Units are m $s^{-1}$

Sample sequences of five-day mean circulation maps were shown to illustrate the variability at periods of the order of 10 days or longer.

The atlas mentioned in the Introduction allows daily tracking of individual systems. One example with a long lifetime produced a distinctive cyclonic circulation over the wind tracking region (to 90°E or beyond) which lasted from 11-22 May. The system appeared to be the successor to the Southern Hemisphere member of the

"twin" circulations identified on 5 May by Rao (1980). The system drifted westward at about $4^{\circ}$/day with a relative vorticity amplitude greater than $40 \times 10^{-6}$ $s^{-1}$ on 12-15 May, the time of associated cloud pattern. A local trade wind maximum was found to the south on 14 May. The system weakened continuously after 15 May and the cloud pattern dissipated; the circulation's latitude varied from $15^{\circ}$S (17 May) to $4^{\circ}$S (22 May), never crossing the equator.

Finally, it is noted that much observational and theoretical work remains to be done on the question of transients propagating across the equator. Preliminary inspection of the atlas maps (Young et al, 1980) shows no clear examples. A possible exception is the "onset" over the Arabian Sea: the Somali Jet was established at half strength on 8 June (implying some local forcing) and reached full strength on 15 June, about two days after the cross-equatorial flow reached normal strength and at which time a cold surge was crossing $20^{\circ}$S. It is likely that theoretical work will be required to establish the modes of temporal links between these latitudes. In the meantime, research is progressing on the use of Hovmöller-type space-time diagrams applied to the various wind variables; about 50 have been produced so far, and some were shown in the presentation.

## 4. MEAN FLOW FORCE DYNAMICS

The historical wind data alone is sufficient to estimate the pressure gradient force $\bar{P}$ from the equations of motion if the friction force $\bar{F}$ at 900 mb is known. Since it is known that the friction force at 900 mb is much smaller than at the surface for undisturbed trade flows, this suggests that the large $\bar{P}$ be calculated as a residual, rather than vice-versa.

Using a drag-law formulation for $\bar{F}$, the $\bar{P}$ field was presented: it showed maxima in the southern westerlies and north western Arabian Sea, with a secondary maximum on the poleward flank of the southeast trades. Directions of $\bar{P}$ were similar to those for geostrophic flows except for a more eastward component near the equator. The divergent part of $\bar{P}$ then allows estimation of the 900 mb geopotential field by relaxation (see Figure 4). This field has features similar to those found for the surface pressure field by other investigators. It is expected that results for a more highly resolved grid will be less smooth and show a more pronounced south-to-north isoline crossing the equator near $65^{\circ}$E.

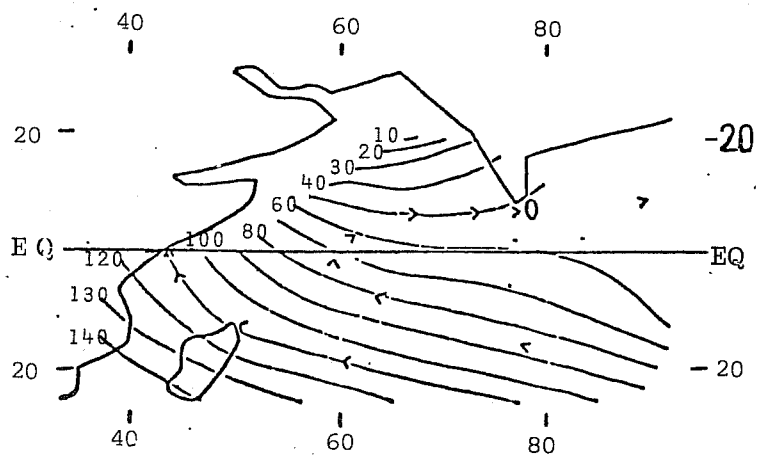


Figure 4 : Preliminary smooth estimate of 900 mb mean geopotential field for established phase of monsoon calculated from cloud wind data. Contour data interval is 10 m.

The estimated force history for mean monsoonal flow across the equator is shown in Figure 5. Starting in the Southern Hemisphere ($20^{o}S$) the trade flow is nearly geostrophic, the acceleration increases toward the equator (where it is essentially centripetal) while Coriolis and pressure gradient forces decrease; downstream from the equator the acceleration is streamwise positive (before the jet core) and then negative (after the jet core) as it decreases in intensity; the greatest friction force is estimated in the jet core. The Rossby number Ro has been separately calculated and shows values in excess of 0.5 between $7^{o}S$ and $9^{o}N$, so that the flow is strongly unbalanced. The Reynolds' number Re peaks at the equator and is a minimum near the jet core, while the Ekman number peaks at the equator, with a general decline toward the poles.

Finally, the dynamic regimes for the entire geographical region were shown. They indicated strong banding parallel to the equator, with a region a few degrees wide with a balance of forces which was quasi-cyclostrophic.

## 5. CONCLUDING REMARKS

These results suggest that the geostationary cloud winds are of research value as II-b sets, even before assimilation into III-b form. They are the major wind set over large areas of the tropical oceans, and over the Indian Ocean appear to possess kinematic and dynamic properties which will give us insight into monsoon mechanisms and provide test fields for numerical simulation experiments.

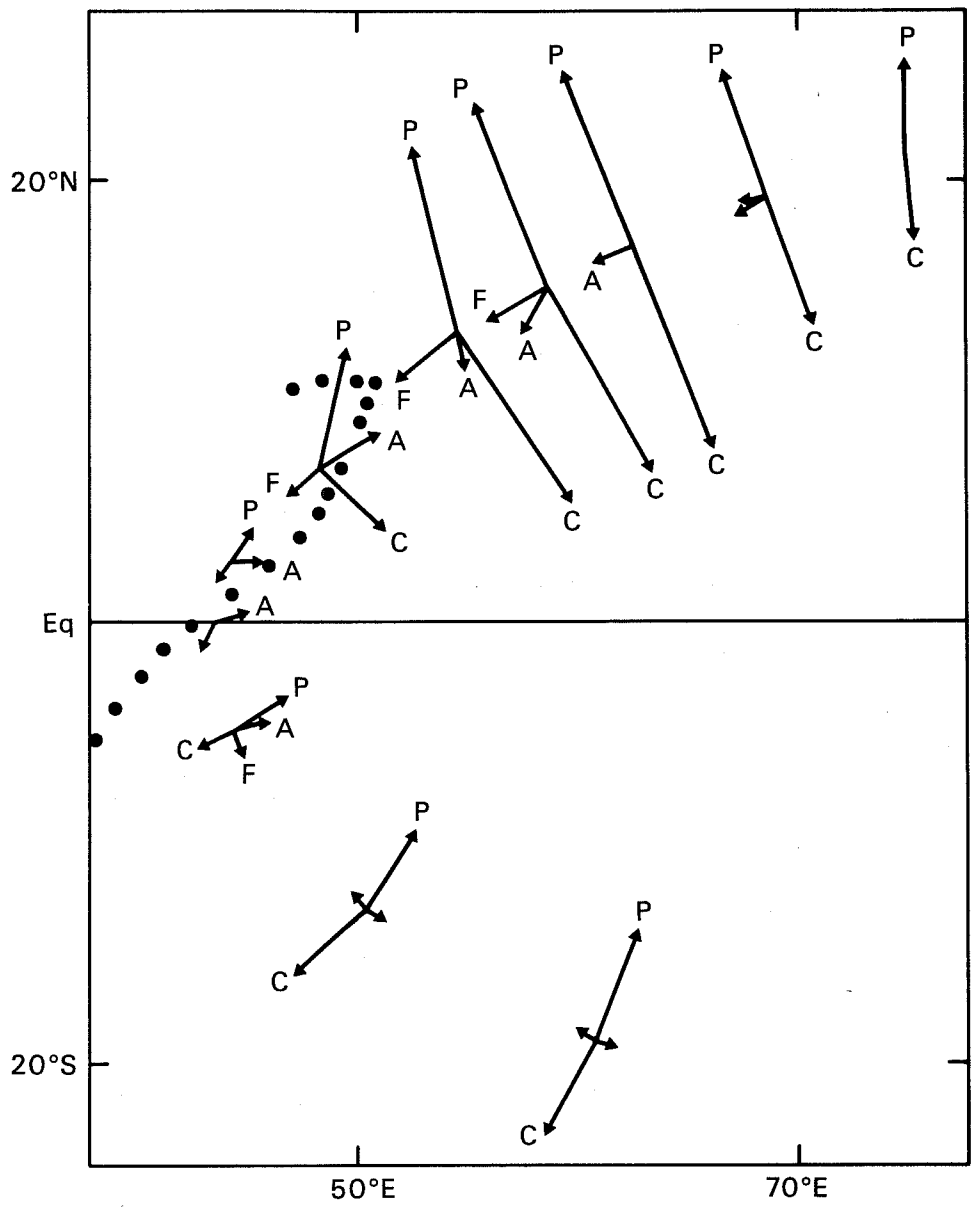


Fig. 5 Equation of motion terms estimated at various locations along a cross-equatorial trajectory through the Somali Jet. $\bar{A}$ = acceleration, $\bar{C}$ = Coriolis force, $\bar{P}$ = pressure gradient force, $\bar{F}$ = friction force. All forces are per unit mass.

ACKNOWLEDGEMENTS

In addition to those mentioned in the text, thanks go to V.E. Suomi for his early faith in the fruits of this wind set, and to numerous FGGE and MONEX wind trackers. Financial support for the winds and the analyses shown here was by NOAA contract 7-35217, and NSF grants ATM 78-21873 and ATM 78-25503 to the University of Wisconsin.

REFERENCES

Rao, P. Krishna, 1980: Twin Tropical Disturbances over the Indian Ocean, Mon. Wea. Rev., 108, 1054-1055.

Young, J.A., Virji, H., Wylie, D.P., and C. Lo, 1980: Summer Monsoon Windsets from Geostationary Satellite Data. Report under N.S.F. Grant ATM 78-21873.